FINITE ELEMENT ANALYSIS OF A STRIP FOOTING ON SAND

Ihab Kachef

A MAJOR TECHNICAL REPORT

in the

Faculty of Engineering

Presented in partial fulfillment of the requirements for
the Degree of Master of Engineering at
Concordia University
Montreal, Quebec, Canada

March 1979

ABSTRACT

FINITE ELEMENT ANALYSIS OF A STRIP FOOTING ON SAND

I. KACHEF

The problem of a strip footing on dense sand is analyzed theoretically by means of a finite element technique. The solution obtained is compared with existing theories as well as the experimental results of Hanna.

The use of Plane strain parameters was found to have a great effect on the theoretical results.

The comparison is made in terms of ultimate bearing capacity, settlement, stress distribution and failure plane beneath the footing. A summary of the comparison is given in the concluding chapter.

ACKNOWLEDGEMENTS

I wish to express my sincere gratitude to Dr. A.M. Hanna, Department of Civil Engineering, Concordia University, for his advises, guidance and encouragement.

I am thankful to Mr. H. Keira, Project Eng. at Rousseau Sauvé Warren, Montreal, Quebec, for his assistance.

Thanks go also to Mr. G. Boulos for his help in the Drawings and Daneta Stanke who typed this report.

TABLE OF CONTENTS

LIST OF FIGURES

LIST OF TABLES

NOTATIONS

a	Reciprocal of the initial tangent modulus
B	Width of footing
b	Reciprocal of the asymptotic value of stress difference
D	Depth of footing
d	Parameter expressing the rate of change of γi with strain
Ei	Initial tangent modulus
Et	Tangent modulus
F	The rate of change of γi with σ_3
f	Value of tangent Poisson's ratio at zero strain
G	Value of γi at one atmosphere
K	Modulus number
Nc, Nq, Nγ	Dimensionless bearing capacity factors
n	Exponent
Pa	Atmospheric pressure
q_u	Ultimate bearing capacity per unit area
Rf	Failure ratio
σ_3	Minor principal stress (confining pressure)
$(\sigma_1 - \sigma_3)$	Stress difference
$(\sigma_1 - \sigma_3)f$	Stress difference at failure

$(\sigma_1 - \sigma_3)p$	Stress difference for plane strain
$(\sigma_1 - \sigma_3)t$	Stress difference for triaxial
$(\sigma_1 - \sigma_3)u$	Asymptotic value of stress difference
ϕ	Angle of internal friction
ϕp	Angle of internal friction for plane strain
ϕt	Angle of internal friction for triaxial strain
γ	Unit weight of soil
γi	Initial tangent modulus
γt	Tangent Poisson's ratio
εa	Axial strain
εr	Radial strain
εv	Volumetric strain

Chapter I

INTRODUCTION

Foundation problems require two different types of study; one deals with the ultimate bearing capacity of the soil under the foundation and the second is concerned with the limit of the deformation.

Analysis of ultimate bearing capacity leads to the determination of the load under which a foundation with given dimensions and depth sinks indefinitely into the soil, i.e. the foundation failure in shear associated with plastic flow of soil material underneath the foundation.

The study of the limiting deformation reveals loading conditions that cause such deformation of the soil. The corresponding total and differential settlements of the structure should not exceed the limits of the allowable deformation for stability function and aspects of construction; these are two independent foundation stability requirements which must be met simultaneously.

The ultimate bearing capacity problem may be solved; numerically by using for example the finite element method or experimentally by testing small and large scale models.

The main objective of this study is to deduce the ultimate bearing capacity of a strip footing on a dense sand layer using a finite element analysis. The results are compared to those offered by available theories and the experimental data of Hanna (1978).

Furthermore a stress strain curve for the plane strain

condition was developed based on the triaxial test results of Hanna.

Chapter 2

REVIEW OF PREVIOUS WORK ON THE ULTIMATE BEARING CAPACITY

2.1 General

The ultimate bearing capacity is defined as the average value of the ultimate contact pressure or stress, or load intensity transmitted by the base of the footing of the foundation to the soil causing the soil mass to rupture or fail in shear. If the load / settlement curve does not exhibit a peak load (Local shear failure), it is defined as the load at which the curve passes into a steep and fairly straight tangent.

If the pressure on a foundation is steadily increased to the value "q_f", the soil in the vicinity of the foundation changes from the state of elastic equilibrium to the state of plastic equilibrium. The change starts at the edge of the foundation, gradually spreading downwards then outwards on each side of the foundation. Eventually, all the soil between the failure surfaces and the ground level reaches the state of plastic equilibrium and complete shear failure takes place with the foundation breaking into the soil.

In case of dense sand the strain prior to failure will be relatively small and the pressure settlement relationship will be of the form demonstrated in Fig. 1 . The ultimate bearing capacity is well defined and failure of this type is referred to as general shear failure(Fig. 2.a). On the other hand, in case of loose sand, the strain prior to failure will be relatively high and the pressure-settlement relationship will be

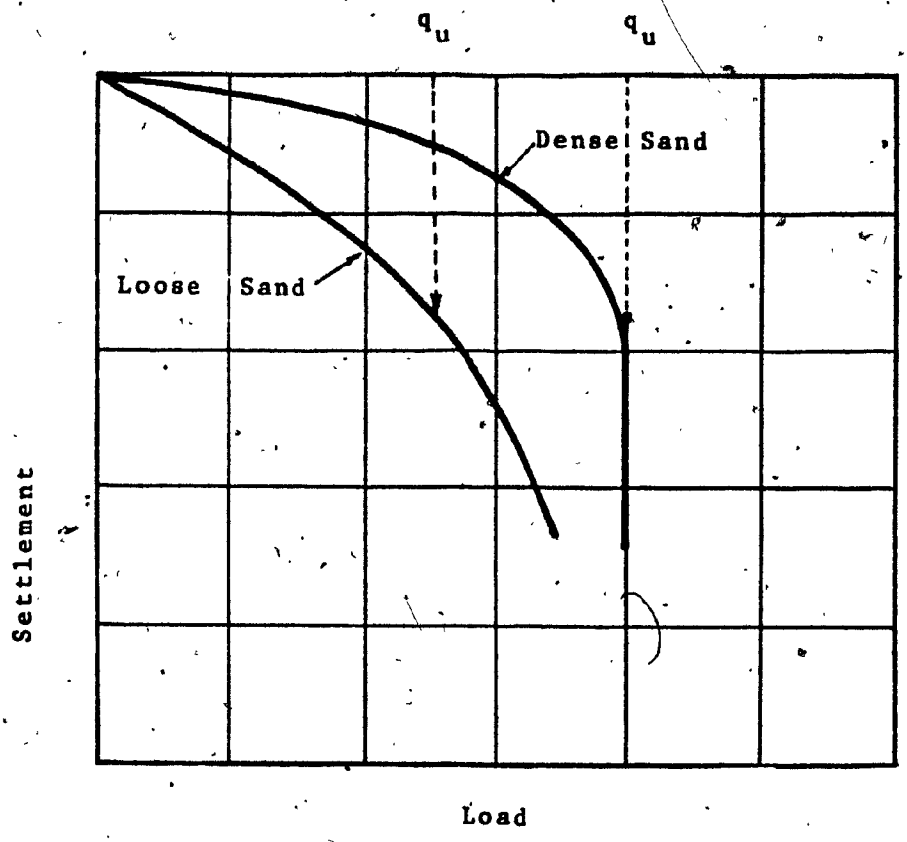

FIG. 1. LOAD SETTLEMENT CURVE

as shown in Fig. 1 . In this case, large settlement, which would be unacceptable in practice, occurs before plastic equilibrium is fully developed and failure is taken arbitrarily at a point where the curve becomes relatively steep and straight; failure of this type is refetred to as local shear failure.

2.2 Mode of Failure

1- General shear failure

This is characterized by the existence of a well defined failure pattern, which consists of a continuous slip surface from one edge of the footing to the ground surface. In stress controlled conditions, under which most foundation operate, failure is sudden and catastrophic; it takes place by rotation and tilting as shown in Fig. 2a.

2- Punching shear failure

This is characterized by a failure pattern that is not easily observed. As the load increases, the vertical movement of the footing is accompanied by compression of the soil immediately underneath. The soil outside the loaded area remains relatively unaffected and there is practically no soil movement on the sides of the footing as shown in Fig. 2.b .

3- Local shear failure

This is a transitional mode where the failure pattern consists of a wedge and slip surface which starts

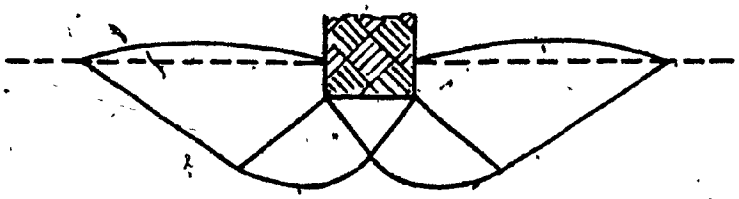

(a)

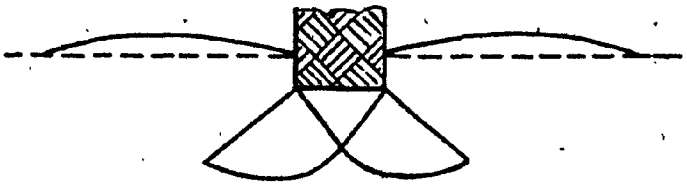

(b)

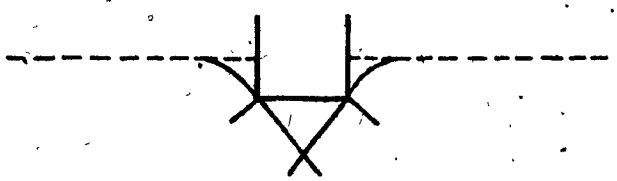

(c)

FIG. 2. MODE OF FAILURE (a) GENERAL SHEAR (b) LOCAL SHEAR (c) PUNCHING SHEAR

at the edge of the footing like in the case of general shear failure. There is a tendency toward soil bulging on the sides of the footing as well as compression under it. Thus the local shear failure retains some characteristics of both general shear and punching modes of failure as shown in Fig.2.c.

2.3 Factors Affecting The Mode Of Failure

The failure mode depends , generally, on the relative compressibility of the soil for given geometrical and loading conditions.

Thus, a footing on the surface of very dense sand will normally fail in general shear, while the same footing on the surface of very loose sand will fail in punching shear. However, the soil type alone cannot define the mode of failure. For example, the footing on very dense sand can fail also in punching shear if the footing is placed at greater depth (Vesic, 1963); or if it is loaded by a transient, dynamic load (Heller, 1964, Selig and Mc Kee, 1961 and Vesic, Banks, Woodard, 1965).

2.4 Discussion

No mathematical approach has been derived for the analysis of such a failure. The several methods developed involve different over simplifications of soil properties and movements. An analysis of the condition of complete bearing capacity failure, usually termed general shear, can be made by assuming

that the soil behaves like an ideally plastic material, and that failure will occur at a point in a soil mass when the shear stress reaches a limiting value dependent on the normal stress (Coulomb, 1776). The concept of plastic material was first developed by Prandtl (1920). In 1924, Reissner extended the Prandtl theory to include cases involving bearing areas which were below the level of the adjacent material by replacing the material located above the level of the bearing area with a uniform surcharge, and assumed that the surcharge had no shear strength. Terzaghi (1943) extended the Prandtl-Reissner solution so that it could be applied to bearing capacity problems in foundation engineering. Terzaghi considered bearing materials which possessed weight, cohesion and friction. He proposed the following general bearing capacity equation for shallow, uniformly loaded strip footings:

$$q_u = cNc + \gamma DNq + \tfrac{1}{2}\gamma BN\gamma \qquad (1)$$

Nc, Nq and Nγ are dimensionless bearing capacity factors that are functions solely of the angle of internal friction of the soil. Since Terzaghi first proposed the general bearing capacity equation, many attempts have been made to improve it. These attempts focussed primarily on the influence of the footing roughness on the values of the ultimate bearing capacity factors, as well as the different assumptions regarding the geometry of the failure zones. Later studies aimed at a more rigorous evaluation of bearing capacity factors, were made by Sokolovski (1960), Meyerhoff (1955,1963), Brinch Hansen (1961,1966,1968) and De Beer (1965). However, the bearing capacity equations developed have the same form as that proposed by Terzaghi with different

values for the bearing capacity factors. Fig.3 compares the values of the bearing capacity factors obtained by Terzaghi and the more recent investigations. Other extensions of the original work by Terzaghi have included considerations of the effects of eccentricity or inclination of loads on the bearing capacity of foundation. Meyerhoff (1953, 1963), studied the effects of eccentricity both theoretically and by means of model tests. Brinch Hansen (1961), presented equations and charts which can be used to calculate the bearing capacity of a footing acted upon by an inclined and/or eccentric loading. Brinch Hansen(1968),extended his previous work to include the effects of inclination of the footing base and of the ground surface on bearing capacity. Meyerhof, (1957)presented equations and charts to determine the bearing capacity of footings on slopes, and proposed equations which can be used to take into account the effect of a high water table on the bearing capacity. Applications of theoretical plasticity methods to problems of engineering interest, and which incorporate discussion of the behaviour of real soil under similar laboratory or field conditions, are limited. West and Stuart, (1965), with greater physical awareness have applied numerical methods to interfering surface footings on sand and have achieved a fair correlation with experimental results.

Berazentzev, (1965) and Mintskovsky, (1965) have also given consideration to the foundation problem, while Gorbunov-Passadov, (1965) has investigated the zone immediately beneath a footing under failure loading.

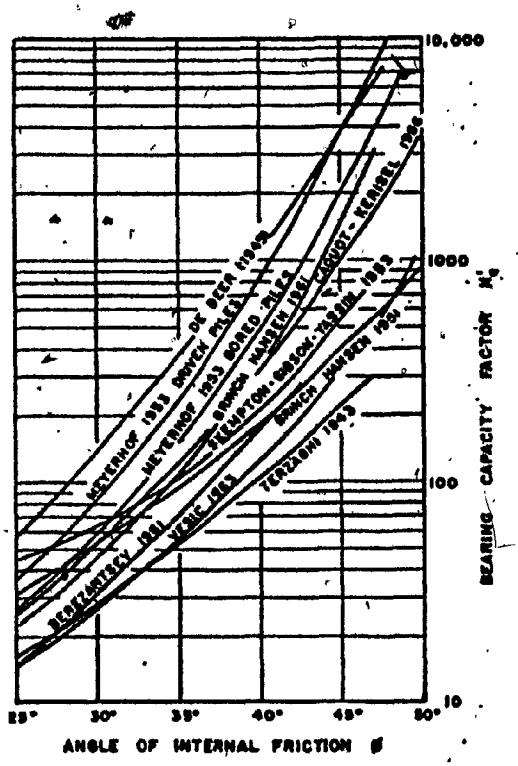

FIG. 3- COMPARISON BETWEEN THEORETICAL AND TEST RESULTS

Chapter 3

NONLINEAR ANALYSIS OF STRESS-STRAIN RELATION

3.1 General

Many problems in soil mechanics are concerned with stresses and deformations in the soil due to boundary and body forces. The theories of elasticity and plasticity have been used to solve certain problems. However, because of computational difficulties, the number of such solutions is limited even for cases in which the stress-strain characteristics of the soil are ideal. The finite element method combined with the availability of high-speed electronic computers made it feasible to perform the analysis for both linear and nonlinear stress strain characteristics.

3.2 The Finite Element Method

The finite element analysis is done by assuming the continuum to be divided into elements. These elements are interconnected at nodal points, and a stiffness matrix equation relating the forces and the deflections at the nodal points is developed. The finite element consists of the following basic operations:

1- Development of a Stiffness matrix of an arbitrary element with respect to a convenient local coordinate system.

2- Development of a transformation matrix (constraint matrix) to transform the stiffness matrix from the local coordinate system to a generalized coordinate system.

3- Generating the final stiffness matrix over the entire assemblage, taking into account the boundary forces, body

forces and deflections.

4- Solution of the system of simultaneous equations. Three conditions must be satisfied in the theory of finite-element analysis in order to develop the stiffness matrix equation:

1- The deformations of adjacent elements must be compatible.

2- The forces acting on the element must be in equilibrium

3- The displacements of each element as a result of the applied forces must be consistent with the Physical properties of the material.

3.3 Nonlinear Stress Analysis By Finite Element

In order to perform a nonlinear stress analysis of soils it is necessary to describe the stress strain behavior of the soil in quantitative terms, and to develop techniques for incorporating this behavior in the analysis. The nonlinear behavior may be approximated in the finite element analysis by assigning a different modulus value to each of the elements over which the soil is subdivided for the purpose of analysis. The modulus value assigned to each element is selected on the basis of the stresses or strains in each element. Because the modulus values depend on the stresses and the stresses in turn depend on the modulus values, it is necessary to make repeated calculations to insure that the modulus values and the stress conditions correspond for each element in the system. Two techniques for approximate stress analysis are shown in Fig.4.

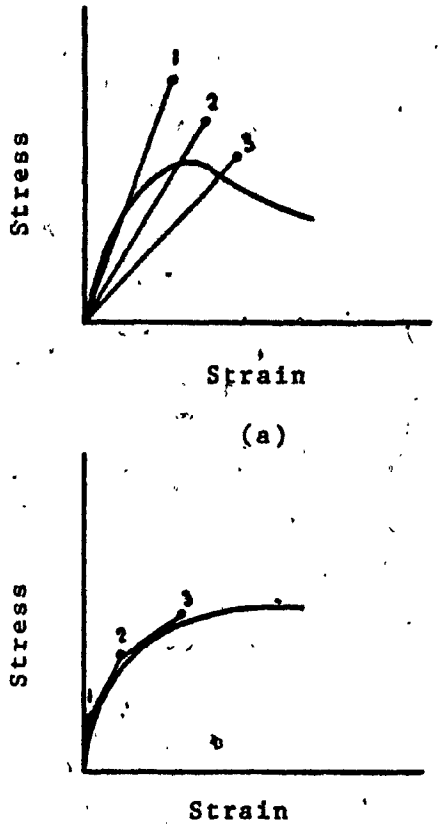

FIG. 4. NONLINEAR STRESS-STRAIN ANALYSIS OF SOILS BY FINITE ELEMENT

Fig. 4.a represents an iterative procedure in which the same change in external loading is analyzed repeatedly. At the end of each iteration, the values of stress and strain within each element are checked to determine if they satisfy the appropriate nonlinear relation between stress and strain. If the values of stress and strain do not correspond, a new modulus value is selected for that element and the iteration is carried through. In the incremental procedure shown in Fig. 4.b., the change of loading is analyzed in a series of steps or increments. At the begining of each new increment of loading, an appropriate modulus value is selected for each element on the basis of the stress or strains values in that element. Thus, the nonlinear stress-strain relationship is approximated by a series of straight lines.

The principal advantage of the incremental procedure is that initial stresses may be readily accounted for. It also has the advantage that, in the process of analyzing the effect of a given loading, stresses and strains are calculated for smaller loads as well. The shortcoming of the incremental procedure is that it is not possible to simulate a stress-strain relationship in which the stress decreases beyond the peak. To do so would require use of a negative value of modulus, and this can not be done with the finite element method. The accuracy of the incremental procedure may be improved if each load increment is analyzed more than once. In this way it is possible to improve the degree to which the linear increments approximate the nonlinear soil behavior.

3.4 Nonlinear Stress-Strain Formulation For Soils

The stress-strain behavior of soil depends on many factors, including density, water content, structure, particle size, drainage conditions, strain conditions (i.e. plane strain, triaxial), duration of loading, stress history, confining pressure and shear stress. It may be possible to account for these factors by selecting soil specimen and testing conditions which simulate the corresponding field conditions. Even when this procedure is followed, it is commonly found that the soil behavior over a wide range is nonlinear, inelastic, and dependent upon the magnitude of the confining pressure employed in the tests. A simplified practical nonlinear stress-strain relationship used with finite element, Duncan & Chang (1970) is described in the following sections

3.4.1 Nonlinearity

Kondner (1963) has shown that the nonlinear stress-strain curves for both clay and sand may be approximated by a hyperbola with a high degree of accuracy. The hyperbolic equation proposed by Kondner is

$$(\sigma_1 - \sigma_3) = \frac{\varepsilon_a}{a + b\varepsilon} \qquad (2)$$

in which σ_1 and σ_3 = major and minor principle stresses; ε_a = axial strain; and a & b= constants whose values may be determined experimentally. In Fig 5.(a), a is the reciprocal of the initial tangent modulus Ei and b is the reciprocal of the asymptotic value of stress difference which the stress-strain curve approaches at infinite strain $(\sigma_1 - \sigma_3)$ ult.

The values of the coefficient a and b may readily be determined if the stress-strain data are plotted on transformed axes as shown in Fig 5.(b). When eq. 1 is rewritten in the following form

$$\frac{\varepsilon_a}{\sigma_1 - \sigma_3} = a + b\varepsilon_a \qquad (3)$$

it may be noted that a and b are respectively, the intercept and the slope of the resulting straight line.

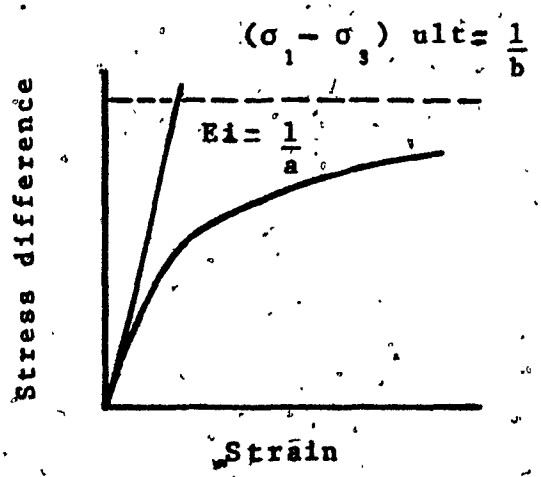

FIG. 5.a. HYPERBOLIC STRESS-STRAIN CURVE

The asymptotic value may be related to the compressive strength by means of a factor Rf as shown by

$$(\sigma_1 - \sigma_3)f = Rf \cdot (\sigma_1 - \sigma_3)u \qquad (4)$$

in which $(\sigma_1 - \sigma_3)f$ = the stress difference at failure; $(\sigma_1 - \sigma_3)u$ the asymptotic value of stress difference; and Rf the failure ratio which has a value less than unity. By expressing the parameters a and b in terms of the initial tangent modulus value and the compressive strength Eq. 2 may be rewritten as

$$(\sigma_1 - \sigma_3) = \frac{\varepsilon_a}{\left[\frac{1}{Ei} + \frac{\varepsilon_a Rf}{(\sigma_1 - \sigma_3)f}\right]} \qquad (5)$$

This hyperbolic representation of the stress-strain curves developed by Kondner has been found to be a convenient and useful means of representing the nolinearity of soil stress-strain behavior.

3.4.2 Stress Dependency

Except in the case of unconsolidated-undrained tests on saturated soils, both the tangent modulus value and the compressive strength of soils have been found to vary with the confining pressure employed in the tests. Experimental studies by Janbu (1963) have shown that the relationship between initial tangent modulus and confining pressure may be expressed as

$$Ei = KP_a \left(\frac{\sigma_3}{Pa}\right)^n \qquad (6)$$

In which Ei = the initial tangent modulus; σ_3 = the minor principal stress; Pa = atmospheric pressure expressed in the same pressure units as Ei and σ_3; K = a modulus number

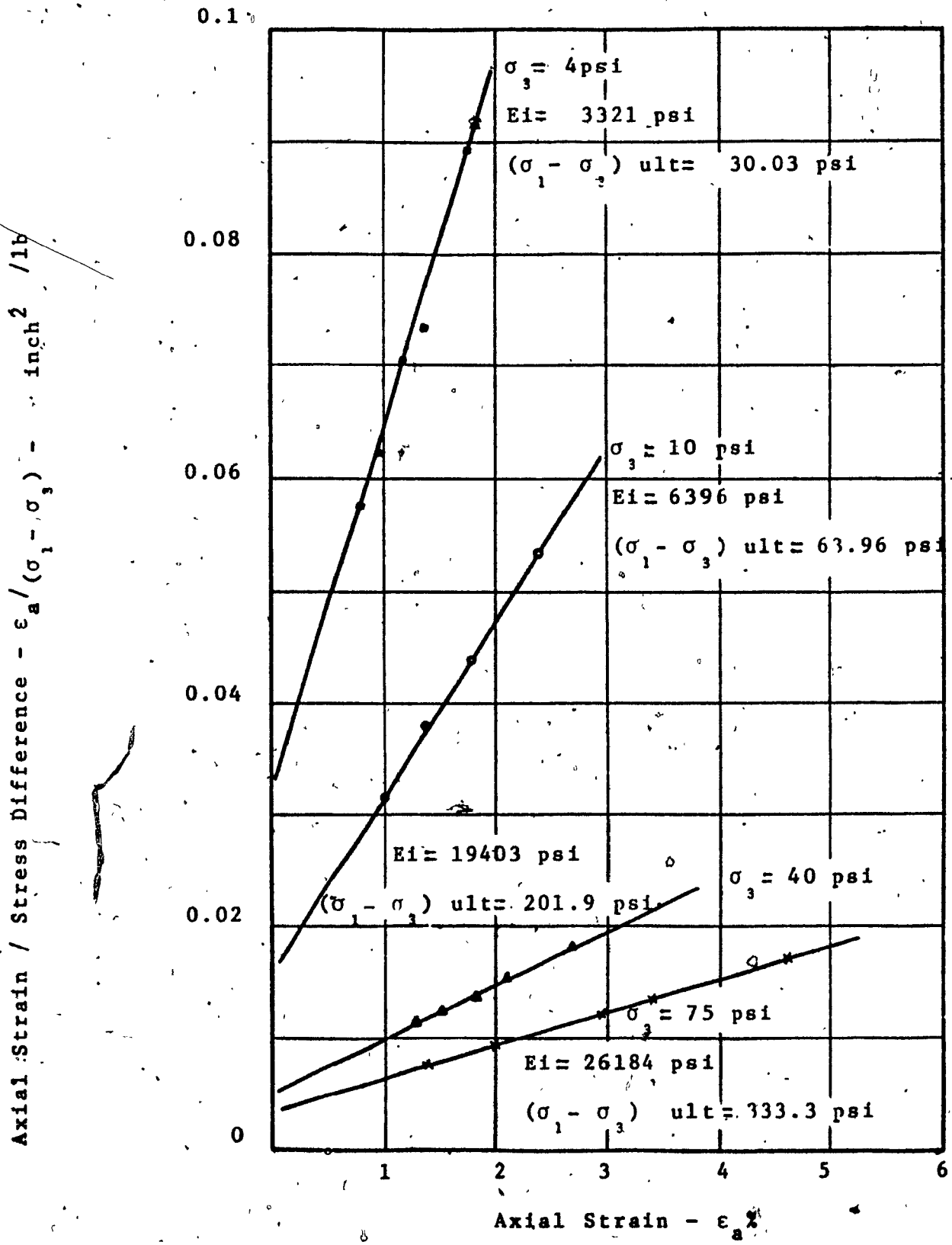

FIG. 5.b. TRANSFORMED STRESS-STRAIN CURVE

and n = the exponent determining the rate of variation of Ei with σ_3. Values of K and n can be determined from the results of a series of tests by plotting the values of Ei against σ_3 on log - log scales and fitting a straight line to the data as shown in Fig. 6. Should it be assumed that failure will occur with no change in the value of σ_3 the relationship between compressive strength and confining pressure may be expressed conveniently in terms of the Mohr-Coulomb failure criterion as

$$(\sigma_1 - \sigma_3)_f = \frac{2c \cos \phi + 2\sigma_3 \sin \phi}{1 - \sin\phi} \qquad (7)$$

in which c and ϕ = the Mohr-Coulomb strength parameters. Eqs. 6 and 7, in combination with Eq. 3 provide a means of relating stress to strains by means of the five parameters K, n, c, ϕ, and Rf.

3.4.3 Tangent Modulus Value

Duncan and Chang (1970) have developed an expression for the tangent modulus which is employed very conveniently in incremental stress analysis. The expression developed by Duncan and Chang was

$$Et = \left[1 - \frac{Rf\ (1-\sin\phi)(\sigma_1 - \sigma_3)}{2c\cos\phi + 2\sigma_3 \sin\phi}\right]^2 Kp_a \left(\frac{\sigma_3}{p_a}\right)^n \qquad (8)$$

The usefulness of Eq. 8 lies in its simplicity with regard to two factors.

1- The tangent modulus is expressed in terms of stresses only so it may be employed for analysis of problems involving any arbitrary initial stress conditions

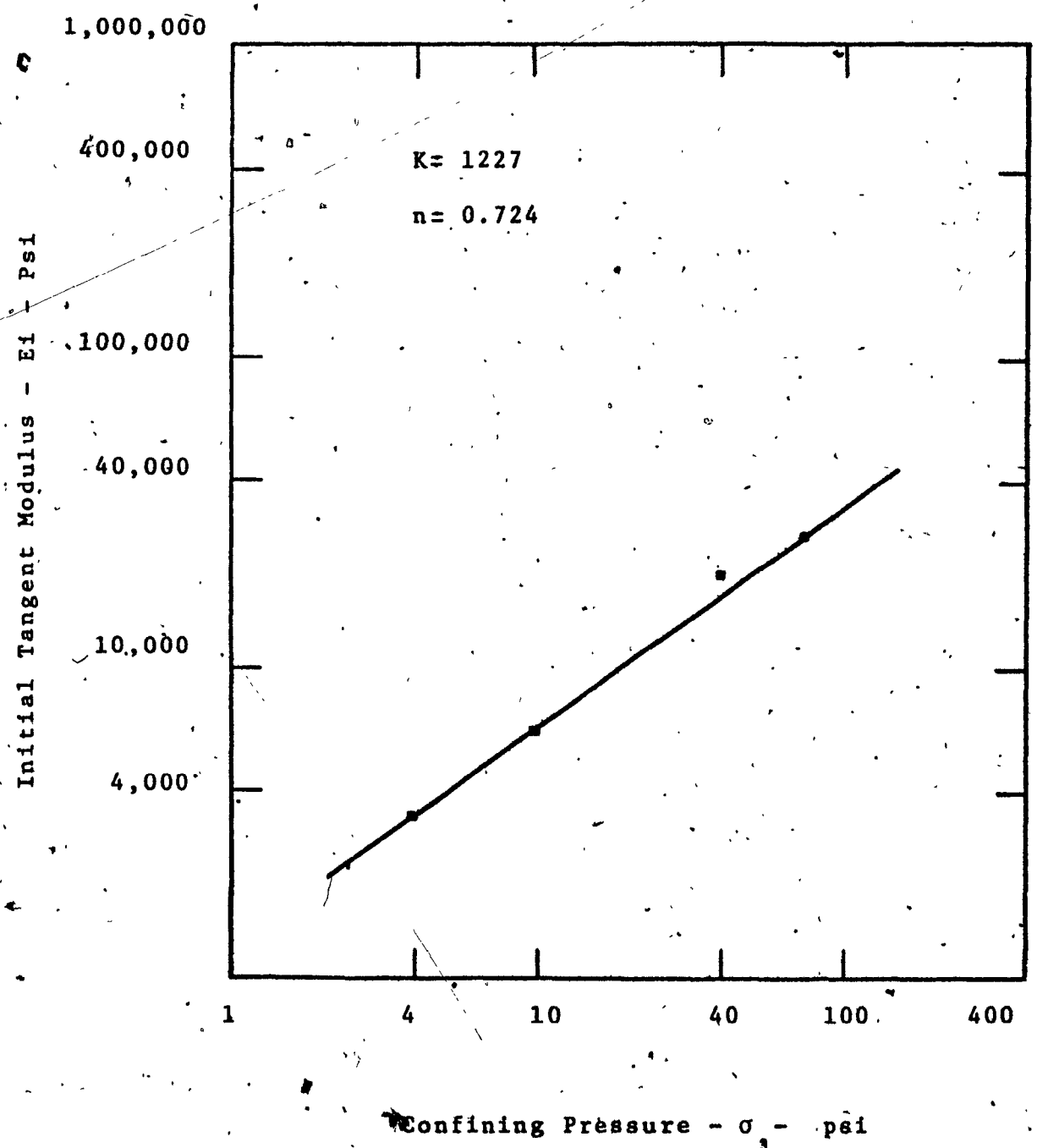

FIG. 6. VARIATIONS OF INITIAL TANGENT MODULUS WITH CONFINING PRESSURE

2- The parameters involved in this relationship can conveniently be determined from laboratory tests.

It should be pointed out that although the stress-strain relationship has been derived on the basis of data obtained from triaxial tests. It may be used for plane strain problems if appropriate plane strain test results are available.

3.4.4 Tangent Poisson's Ratio

Kulhawy, Duncan and Seed (1969) demonstrated that a hyperbolic equation can be used to describe the nonlinear relationship between the axial and radial strains during triaxial shear tests in the form

$$\frac{\varepsilon r}{\varepsilon a} = f + d\varepsilon r \qquad (9)$$

in which εr = the radial Strain; εa = the axial strain; f = the value of tangent Poisson's ratio at zero strain or the initial tangent Poisson's ratio, γi; d = the parameter expressing the rate of change of γi with strain. The values of γi and d can be determined by plotting the values of $\frac{\varepsilon r}{\varepsilon a}$ against εr and fitting a straight line as shown in fig. 7.

The value of γi was found to vary semilogarithmically in the form of

$$\gamma i = G - F \log \frac{\sigma_3}{Pa} \qquad (10)$$

in which G = the value of γi at one atmosphere; F = the rate of change of γi with σ_3 ; and Pa = atmospheric pressure in the same units as σ_3 the values of G and F can be determined from the results of a series of tests by plotting the values of γi against $\left(\frac{\sigma_3}{Pa}\right)$ on a semi-logscale and fitting a straight

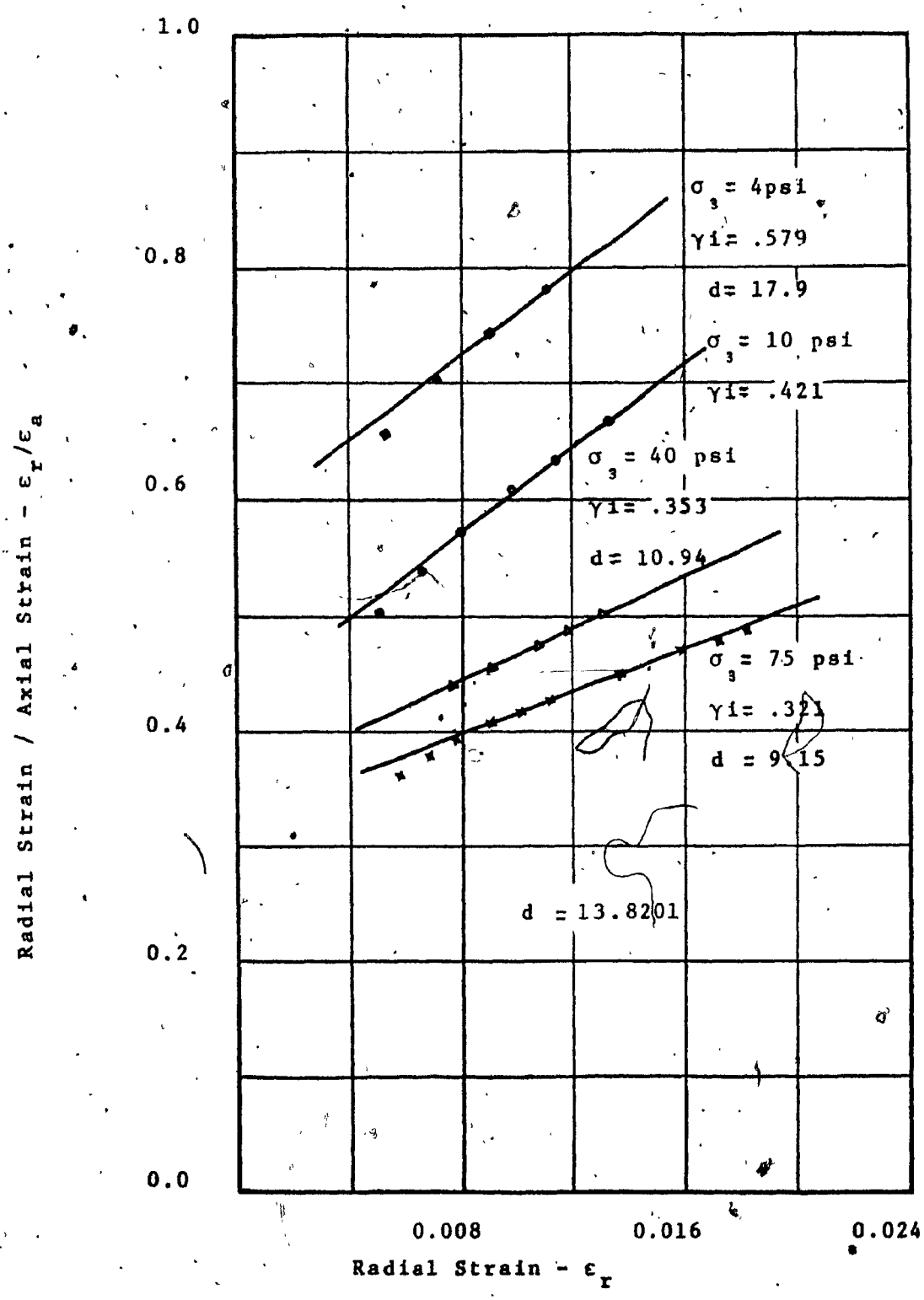

FIG. 7. VARIATION OF RADIAL/AXIAL STRAIN WITH RADIAL STRAIN

line to data as shown in Fig. 8.

Kulhawy and Duncan (1972) showed that the resulting expression for the tangent Poisson's ratio is

$$\gamma t = \frac{G - F \log (\frac{\sigma_3}{Pa})}{(1 - d\varepsilon a)^2} \qquad (11)$$

in which

$$\varepsilon a = \frac{(\sigma_1 - \sigma_3)}{KPa\ (\frac{\sigma_3}{Pa})^n \left[1 - \frac{Rf\ (\sigma_1 - \sigma_3)(1-\sin\phi)}{2c\cos\phi + 2\phi_3 \sin\phi}\right]} \qquad (12)$$

as given by Duncan & Chang (1970). It should be noted that

$$\varepsilon r = \frac{\varepsilon v - \varepsilon a}{2} \qquad (13)$$

Poisson's ratio parameters d, G and F obtained by this method were shown to agree with the experimental results of Whithiam and Kulhawy (1976).

3.5 Program Used

A finite element program developed by F.H. Kulhawy (1969) using the nonlinear stress-strain Formulation for the Soils described previously was used in this study. The program is composed of one principal program LSBUILD and six sub-routines (LAYOUT, LSSTIF, LSQUAD, LST8, BANSOL and LSRESL) it calculates the displacements, deformations and stresses in a dam with a homogenous or composite section constructed on a rigid or compressible foundation. The analysis assumes a state of Plane deformation and isotropic materials. The construction per layer is simulated. Young modulus and Poisson's coefficient vary with the stress state and are recalculated at each iteration for each layer.

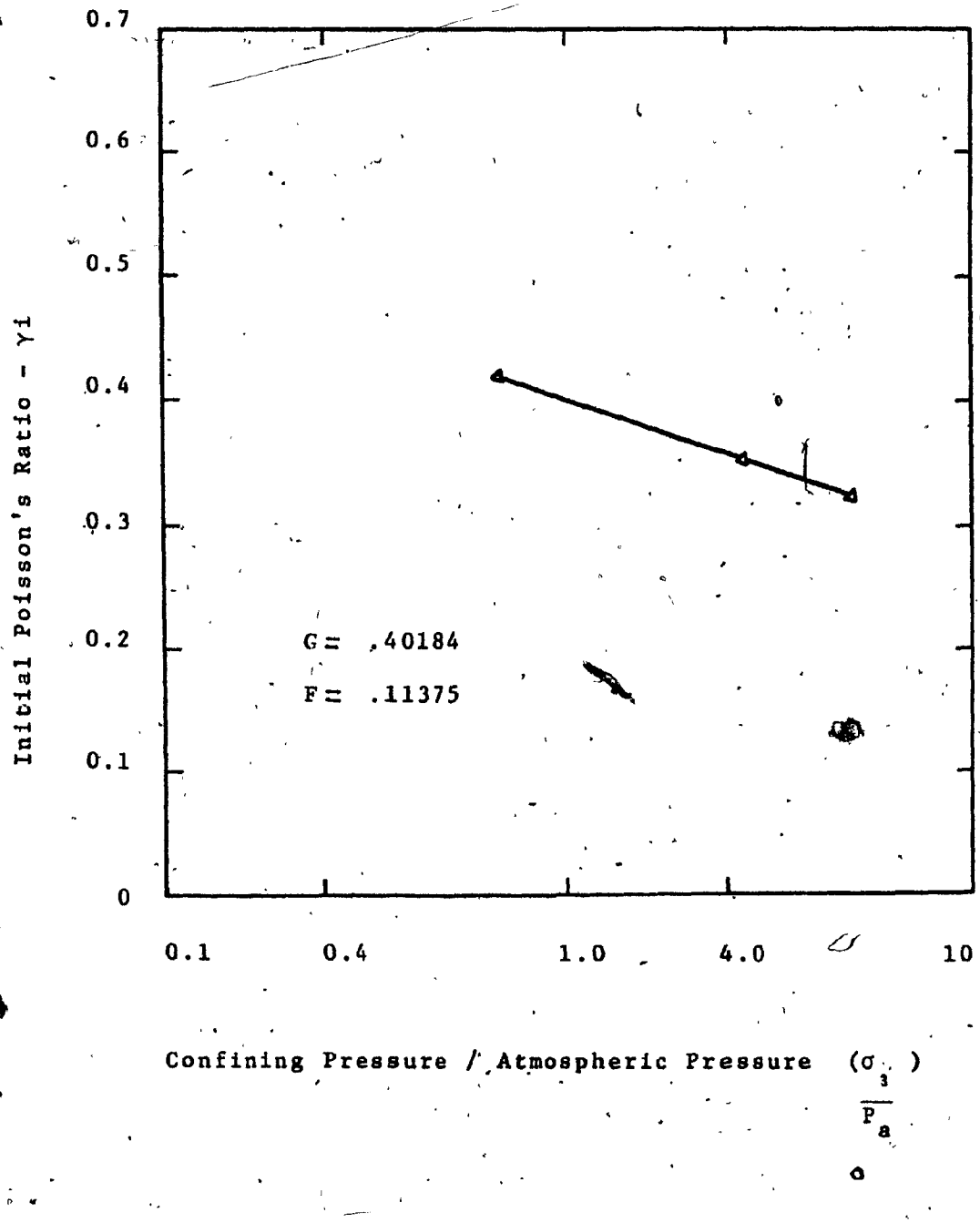

FIG. 8. VARIATION OF INITIAL POISSON'S RATIO WITH CONFINING PRESSURE / ATMOSPHERIC PRESSURE

3.5.1 Program Arrangement

The program LSBUILD control the operations by calling sub-routines when it is necessary..

- LAYOUT analyses the entry data, calculates the initial stresses in the foundation and the initial elastic properties.
- LSSTIF builds the global stiffness matrix from the elements stiffness matrix calculated by LSQUAD. It modifies the global matrix in function of the imposed boundary conditions.
- LSQUAD calculates the stiffness matrix of each quadrilateral element for LSSTIF and LSRESL and calculates the gravity loads applied at the nodes.
- LST8 calculates the stiffness matrix of each of the two triangles composing the quadrilateral element.
- BANSOL calculates the displacements by Gauss elimination.
- LSRESL calculates the deformations and the stresses of each element and recalculates the tangent modulus and the Poisson's coefficient for a new iteration or for the next step in construction.

Chapter 4

RESULTS

4.1 Finite Element Model Description

The 2 inch wide strip footing used is laid on the top of a 20"x24" layer of dense sand. The finite element mesh contains 258 elements and 296 nodal points as shown in Fig. 9. The nodal points all along the vertical boundaries and the bottom horizontal boundary are constrained from either horizontal or vertical movements. The rest of the nodal points including those at the surface are unconstrained.

There is no Provision in the Program to give increments of loads on the footing since the program is designed to calculate stresses and strains in dams. However, the layer construction characteristic of the program is used to provide the necessary load increment. Through six layers with a value of γ at each layer equal to the load increment required divided by the volume of the layer.

The parameters K,n,Rf, ϕ and γ of the load increment layers are assigned high values to avoid any failure occurence.

Six increments of load of 10, 20, 30, 32, 34, 36 psi were applied on the footing respectively.

4.2 Evaluation of the Parameters

The results of the triaxial test results conducted by A. Hanna (1978) on sand samples, shown in Appendix 1, were used to evaluate the parameters K,n,Rf, ϕ, γ, d, G and F.

The stress-strain data in Table 1 are plotted on transformed

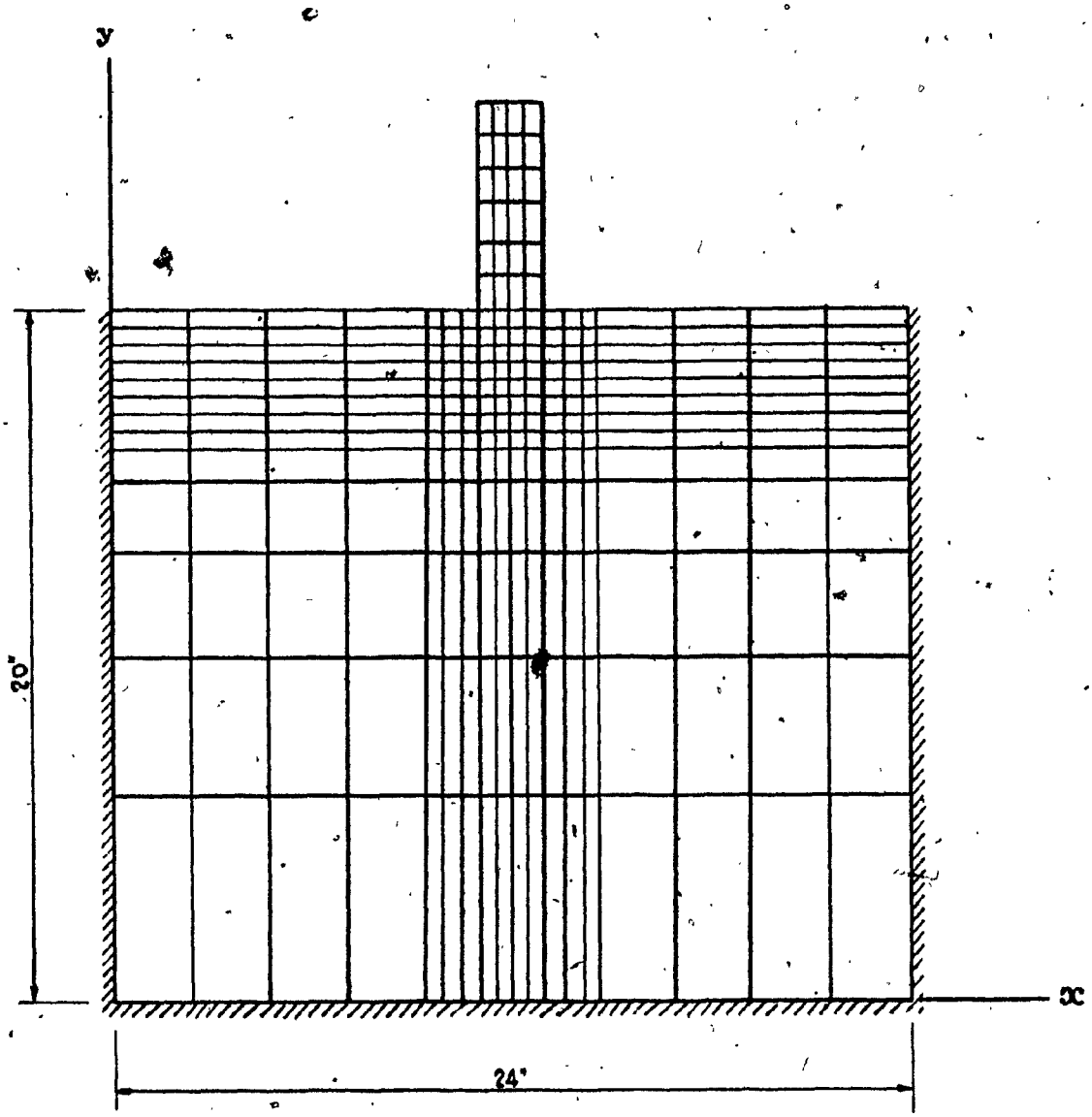

FIG. 9. FINITE ELEMENT MODEL

axes for different confining pressures as shown in Fig. 5.b for the purpose of determinig the values of Ei and $(\sigma_1 - \sigma_3)$ u. A straight line is fitted between a stress level S= 0.7 and S= 0.95 as suggested by Duncan and Chang (1970).

The values of K,n,d,G and F were obtained as discussed previously and are shown in Figs. 6,7 and 8. The first computer run was made using these data. The load settlement curve under the mid-point of the footing is shown in Fig. 10 (case 1). The value obtained in "qu" is higher than the value of 10psi calculated using Terzaghi bearing capacity factors in Eq. 1, but is half the qu value obtained experimentally by Hanna (Fig. 10 - (case 5)). The difference is justified by the use of triaxial test results parameters instead of the plane strain test results which leads to more conservative ultimate bearing capacity values.

4.3 Data Modification To Simulate The Plane Strain Condition

Hansen (1) considered the bearing capacity as a plane strain problem for the infinitely long strip footing considered by Prandtl. In a plane strain case the angle ϕ from triaxial tests tends to be too low. Hansen suggests that

$$\phi \text{ plane strain} = 1.1\ \phi \text{ triaxial} \qquad (14)$$

The above relationship was used to calculate the stress difference $(\sigma_1 - \sigma_3)$ p for the plane strain condition from

$$\sin\phi = \frac{(\sigma_1 - \sigma_3)}{(\sigma_1 + \sigma_3)} \qquad (15)$$

where ϕ = ϕ plane strain for this case calculated from Eq. 14.

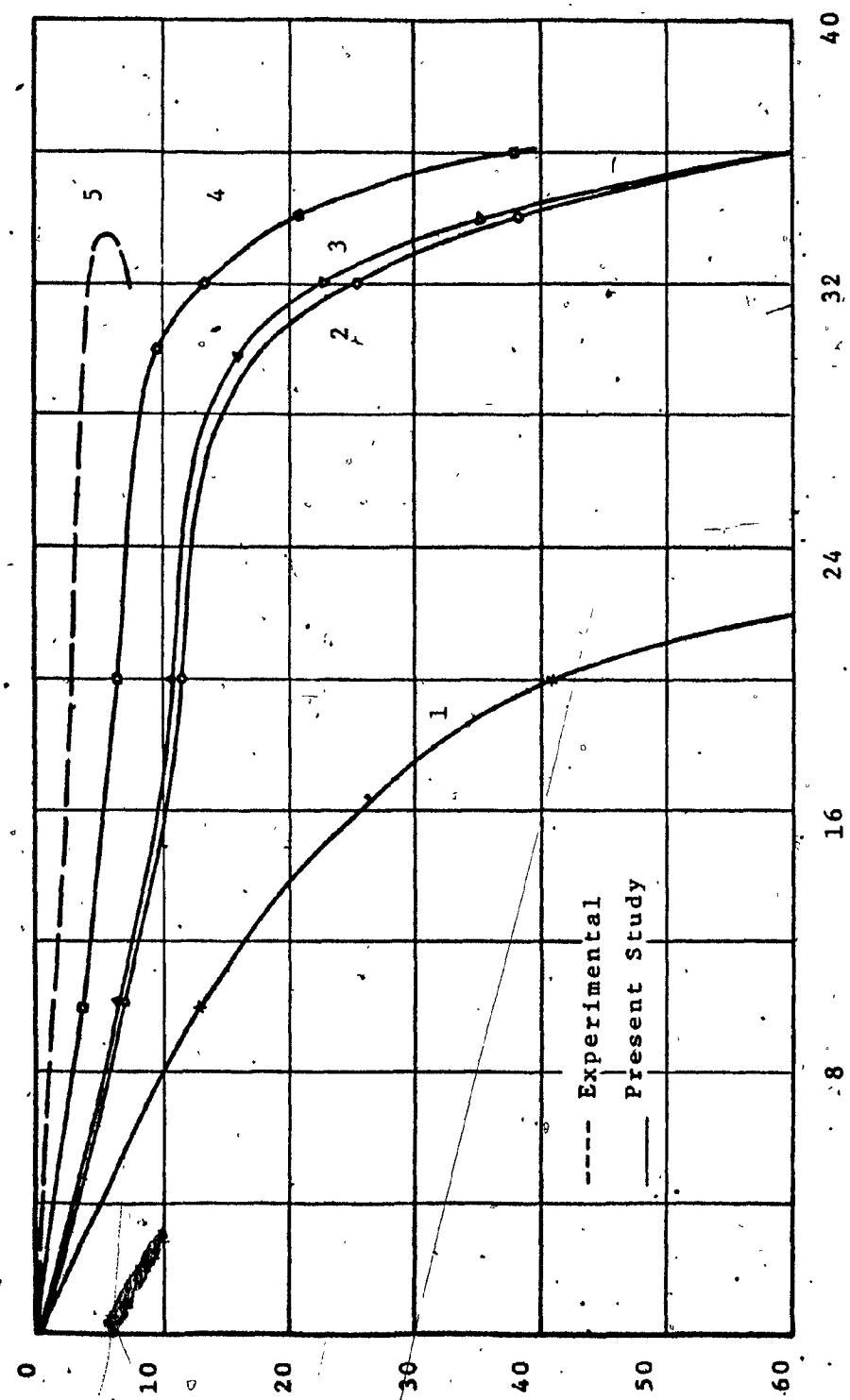

FIG. 10. LOAD SETTLEMENT CURVES

The corresponding calculations to get ϕp and the stress difference $(\sigma_1 - \sigma_3)p$ from triaxial tests stress strain data are shown in Tables 1.a, 1.b, 1.c and 1.d.

Table. 1.a - CONVERTING DATA FROM TRIAXIAL TO PLANE STRAIN

$(\sigma_1 - \sigma_3)_t$	ϵ_t%	ϕ_t	ϕ_p	sin ϕ_p	$(\sigma_1 - \sigma_3)_p$	$e/(\sigma_1 - \sigma_3)_p$	σ_3
90	.6	22.02	25.14	.4248	110.78	0.005416	75
105	.7	24.31	27.76	.4657	130.74	0.005354	"
130	.9	27.6	31.52	.5228	164.33	0.005476	"
172	1.4	32.3	36.9	.6004	225.37	0.006212	"
205	2.0	35.27	40.3	.6467	274.57	0.007284	"
233	2.9	37.47	42.8	.6794	317.87	0.009123	"
243	3.4	38.2	43.62	.6898	333.6	0.010192	"
260	4.6	39.35	44.93	.7062	360.6	0.01275	"
266	5.7	39.74	45.38	.7117	370.3	0.01539	"
267	6.9	39.81	45.46	.7127	372.1	0.01854	"
260	8.6	39.35	44.93	.7062	360.55	0.02385	"
253	9.7	38.88	44.4	.6996	349.33	0.02776	"
243	10.8	38.2	43.62	.6898	333.56	0.03237	"
235	12.0	37.6	42.93	.6811	320.36	0.03745	"

Table 1.b - CONVERTING DATA FROM TRIAXIAL TO PLANE STRAIN

$(\sigma_1 - \sigma_3)_t$	ε_t%	ϕ_t	ϕ_p	sin ϕ_p	$(\sigma_1 - \sigma_3)_p$	$\varepsilon / (\sigma_1 - \sigma_3)_p$	σ_3
35	0.2	17.72	20.23	.3457	42.27	0.00473	40
47	0.3	21.72	24.8	.4194	57.8	0.00519	"
65	0.5	26.63	30.41	.5062	82.	0.0061	"
85	0.8	31.	35.4	.5793	110.2	0.00726	"
110	1.3	35.37	40.4	.6481	147.33	0.0088	"
120	1.5	36.86	42.09	.6703	162.64	0.00922	"
130	1.8	38.24	43.67	.6905	178.5	0.01008	"
135	2.1	38.9	44.42	.6999	186.58	0.01125	"
145	2.7	40.12	45.82	.7171	202.8	0.0133	"
155	3.8	41.26	47.12	.7328	219.4	0.0173	"
158	4.9	41.6	47.5	.7372	224.4	0.0218	"
157	6.0	41.48	47.3	.7349	222.78	0.02705	"
153	6.4	41	46.82	.7292	215.4	0.0297	"
145	8.4	40.12	45.6	.7145	200.21	0.0419	"

Table 1.c - CONVERTING DATA FROM TRIAXIAL TO PLANE STRAIN

$(\sigma_1 - \sigma_3)_t$	ε_t%	ϕ_t	ϕ_p	sin ϕ_p	$(\sigma_1 - \sigma_3)_p$	$\varepsilon / (\sigma_1 \sigma_3)_p$	σ_3
15	0.4	25.4	29	.4848	18.82	0.02125	10
21	0.6	30.8	35.17	.576	27.17	0.02208	"
26	0.8	34.42	39.31	.6335	34.57	0.02324	"
32	1.0	37.98	43.37	.6867	43.83	0.02281	"
37	1.4	40.5	46.25	.7224	52.05	0.02689	"
41	1.8	42.23	48.22	.7457	58.65	0.03069	"
45	2.4	43.81	50	.766	65.47	0.03665	"
48	3.2	44.9	51.27	.78	70.91	0.04512	"
48	3.6	44.9	51.27	.78	70.91	0.05076	"
46	4.9	44.2	50.47	.7713	67.45	0.07264	"
45	6.0	43.8	50	.766	65.47	0.09164	"
43	7.0	43	49	.7558	61.9	0.11308	"

Table 1.d - CONVERTING DATA FROM TRIAXIAL TO PLANE STRAIN

$(\sigma_1 - \sigma_3)_t$	ε_t%	ϕ_t	ϕ_p	sin ϕ_p	$(\sigma_1 - \sigma_3)_p$	$\varepsilon/(\sigma_1 - \sigma_3)_p$	σ_3
5	0.2	22.62	25.83	.4357	6.17	0.0324	4
10	0.4	33.74	38.53	.6229	13.21	0.03028	"
12	0.6	36.87	42.1	.6704	16.27	0.03687	"
14	0.8	39.52	45.13	.7087	19.46	0.0411	"
16	1.0	41.8	47.73	.74	22.77	0.043917	"
17	1.2	42.8	48.87	.7532	24.41	0.04916	"
19	1.4	44.72	51.1	.7782	28.06	0.04989	"
20	1.8	45.6	52.1	.789	29.91	0.06018	"
21	2.2	46.4	52.98	.7984	31.7	0.0694	"
20	3.4	45.6	52.07	.7887	29.86	0.11386	"

A second computer run was made using the same parameters as run no.1 and changing the value of ϕ to ϕ_p; the corresponding load settlement curve is shown in Fig.10 (Case 2).
The ultimate bearing capacity increased considerably in the second run but was still lower than the experimental result of Hanna(Fig. 10-(Case 5)).
A third computer run was made using the modified values of stress difference $(\sigma_1 - \sigma_3)_p$ and ϕ_p and a small increase in q_u was obtained(Fig. 10 (Case 3)). A series of computer runs were made using axial strains decreased by small increments. At a strain decrease of 40%, the ultimate bearing capacity agreed with the experimental value as shown in Fig. 10 (Case 4). However, the predicted value of settlement/width of the footing is higher than the experimental value. This can be justified by the difference between the strain controlled condition of the experiment, and the stress controlled condition represented by the increase of load in the program.
Table (2) summarizes the parameters for the 4 main computer runs which are equivalent to cases 1, 2, 3 and 4 in Fig. 10. The values of the parameters Ei, K and n used in the fourth run are shown in Figs. 11 and 12.

4.4 Analysis

The load settlement curves obtained from both the experimental data and the finite element analysis are shown in Fig. 10.
The use of ϕ_p only with the triaxial test parameters increased

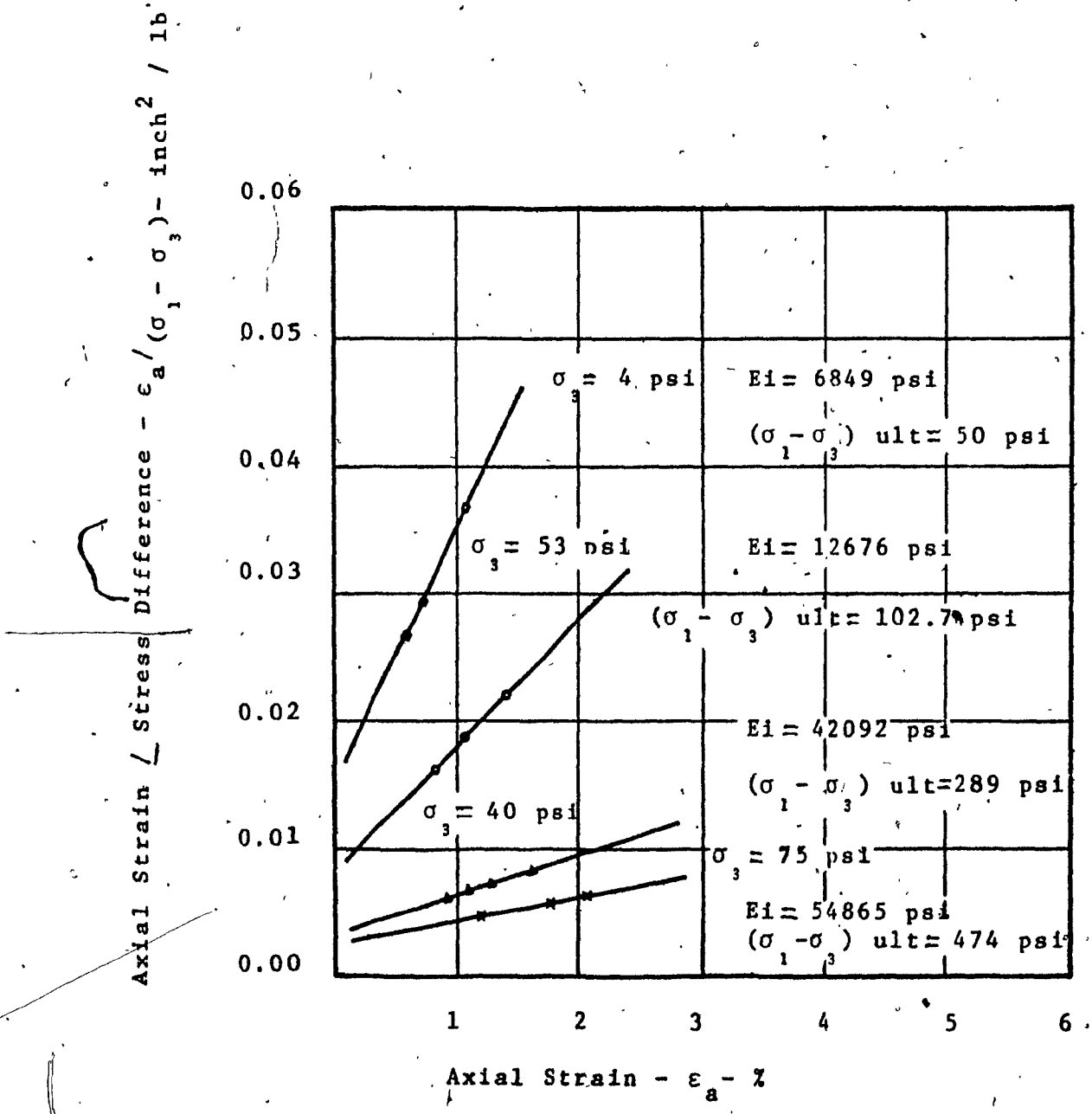

FIG. 11. TRANSFORMED STRESS-STRAIN CURVE FOR PLANE STRAIN CONDITION

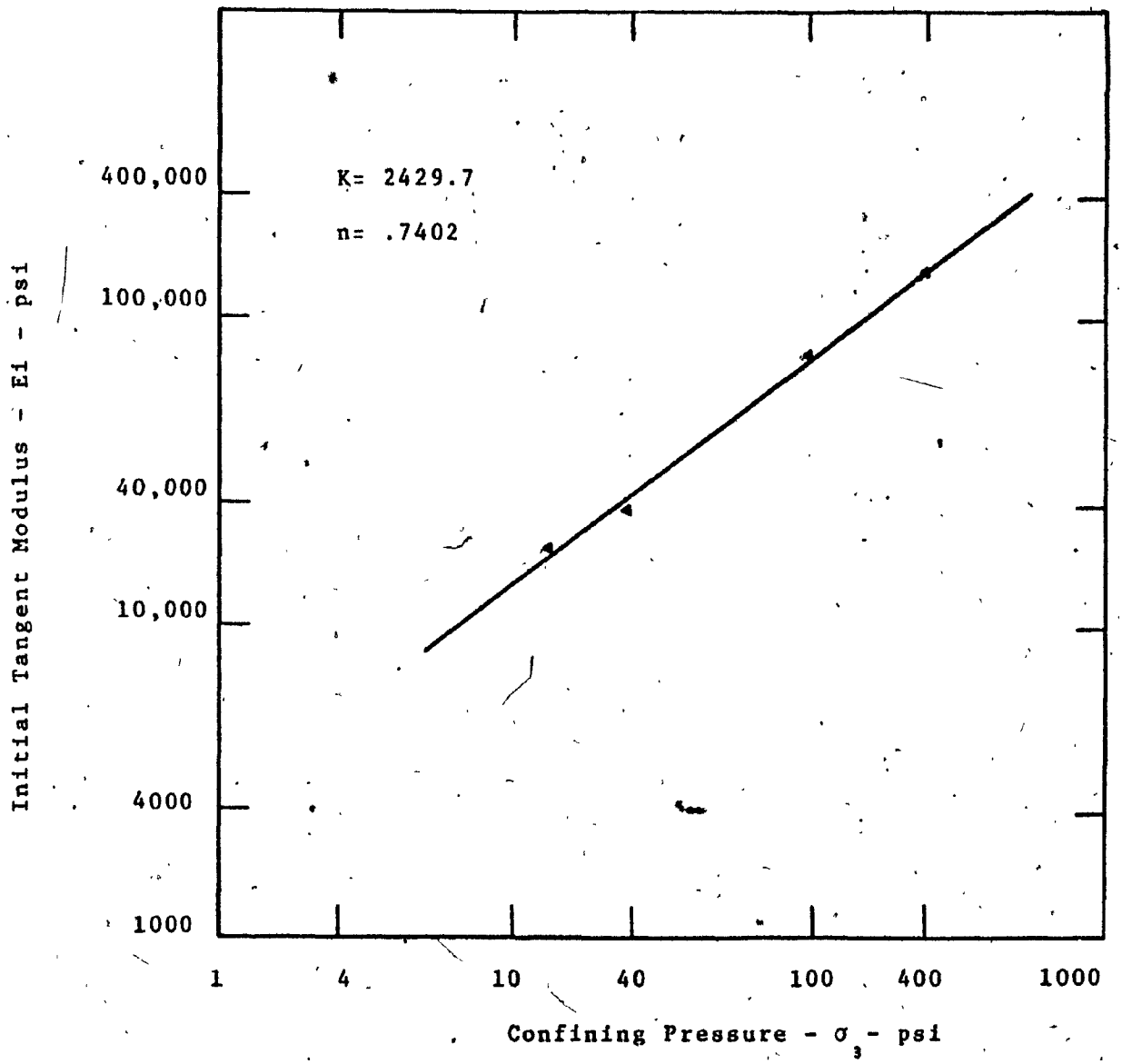

FIG. 12. VARIATIONS OF INITIAL TANGENT MODULUS WITH CONFINING PRESSURE FOR THE PLANE STRAIN CONDITION

Table 2 - SUMMARY OF STRESS STRAIN DATA USED FOR COMPUTER RUNS

Case N°	ϕ	Rf	K	n	d	G	F	γ
1	42°	1	1227	0.724	13.820	.402	.114	104
2	48°	1	1227	0.724	13.8201	.402	.114	104
3	48°	1	1447.7	0.7409	13.8201	.402	.114	104
4	48°	1	2429.7	.7402	13.9201	.402	.114	104

"q_u" by an amount of 38% compared to "q_u" obtained with the use of ϕ_t. A 13% increase in "q_u" was obtained by modifying the stress-strain curve. The value of the settlement/width of the footing decreased from a 44% using ϕ_t to an amount of 17% after modifying the stress-strain curve and using ϕ_p. The stress distribution beneath the footing from the finite element and from Boussinesq equations are shown in Figs. 14 and 15.

In Fig. 14 both the finite element results and the theory agree since the stress-strain relationship is a linear one, i.e. the soil behaves as an elastic material.

The disagreement shown in Fig. 15 is due to the fact that the assumption of the soil as an elastic material used by Boussinesq does not hold after a value of $\frac{1}{3} q_u$ (= 10 psi in ~~this case~~).

A general shear failure mode was obtained in this study as shown in Fig. 16. The failure occured on one side of the footing only. The plane of failure from either the theory or the finite element did not reach the surface of the soil due to the vertical boundary condition. To avoid such boundary conditions, a bigger ratio of B to the distance from the edge of the footing should be taken.

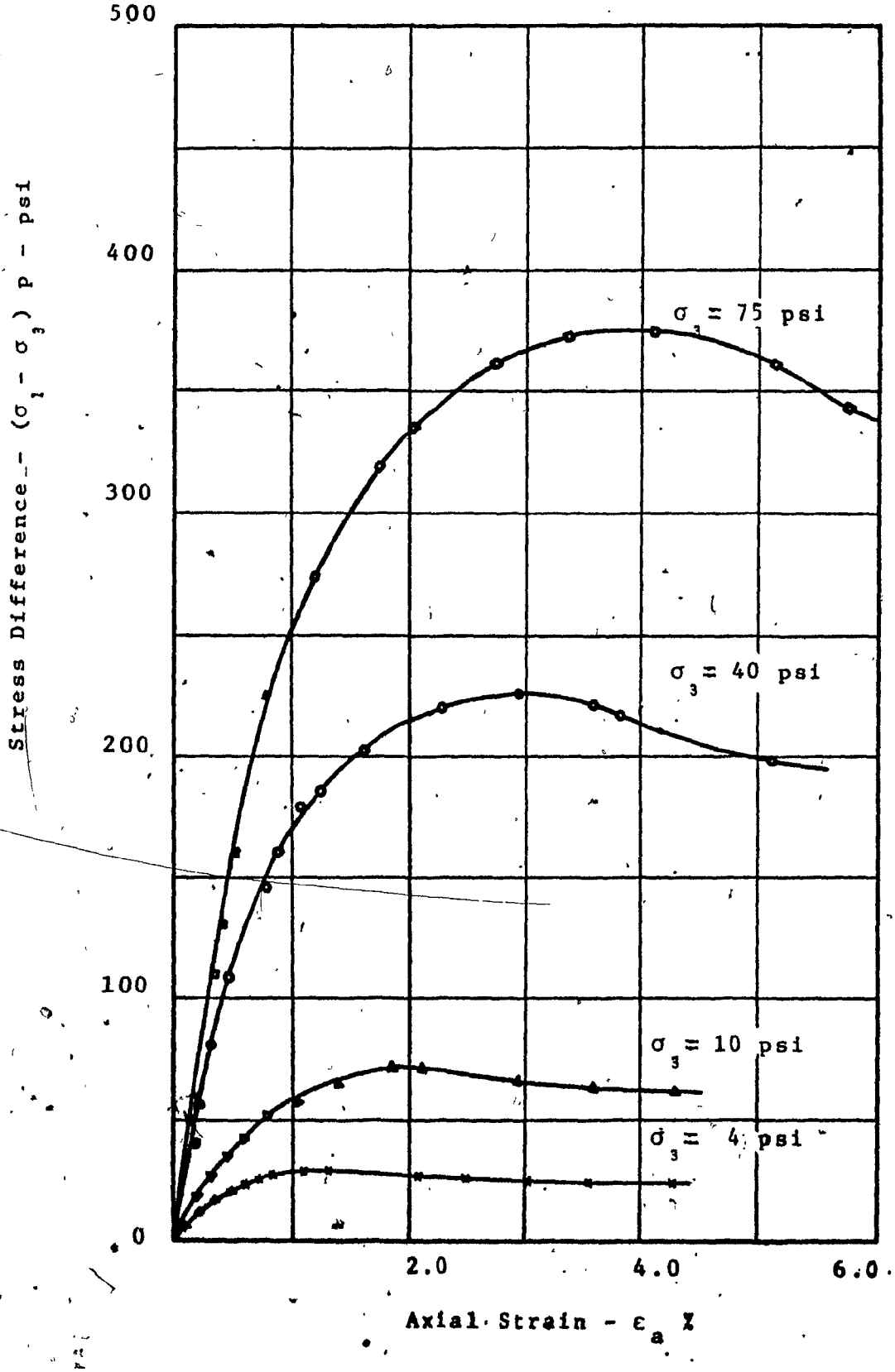

FIG. 13. STRESS-STRAIN CURVES FOR PLANE STRAIN CONDITION

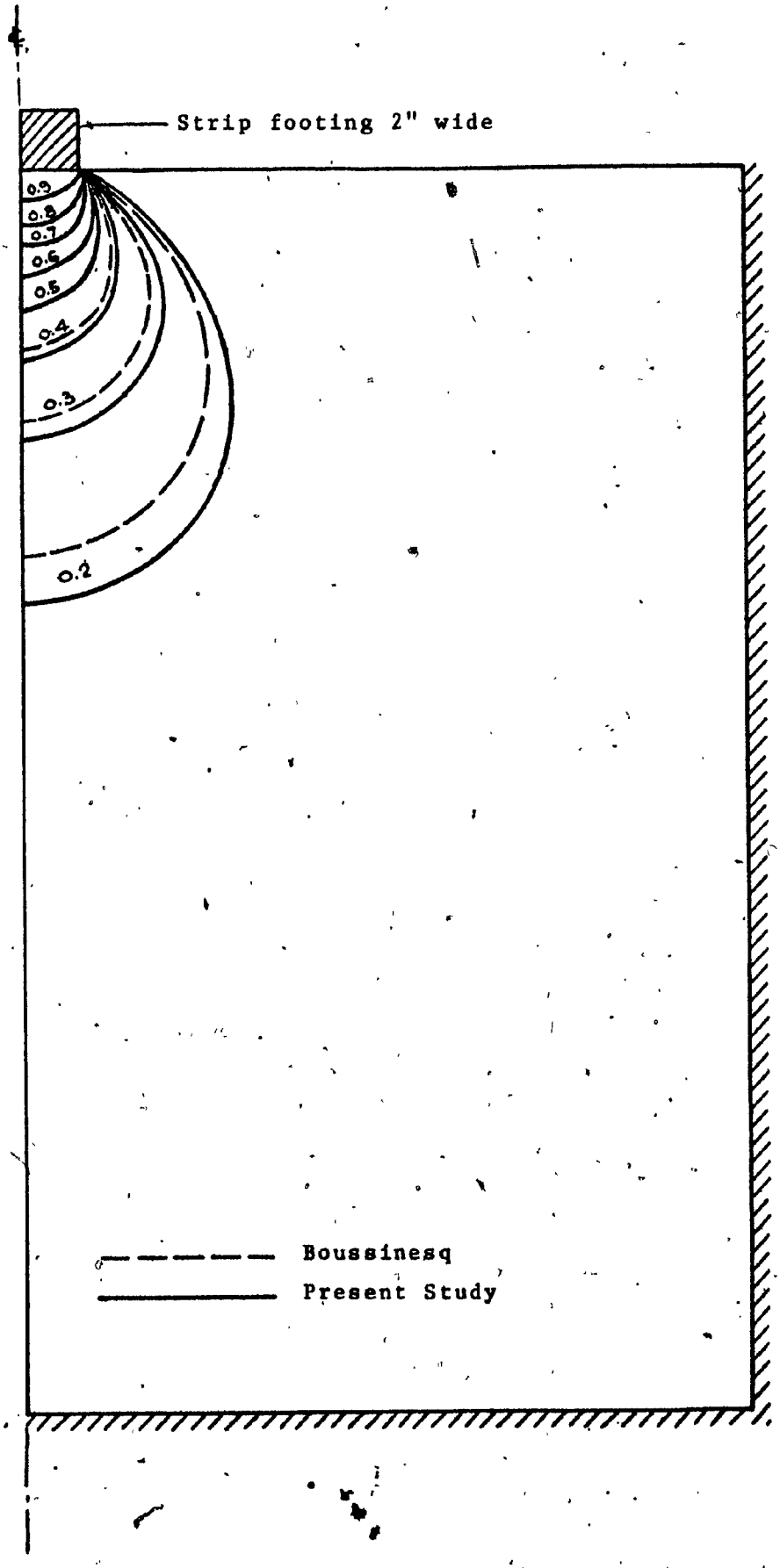

FIG. 14. STRESS DISTRIBUTION BENEATH THE FOOTING AT 10 PSI

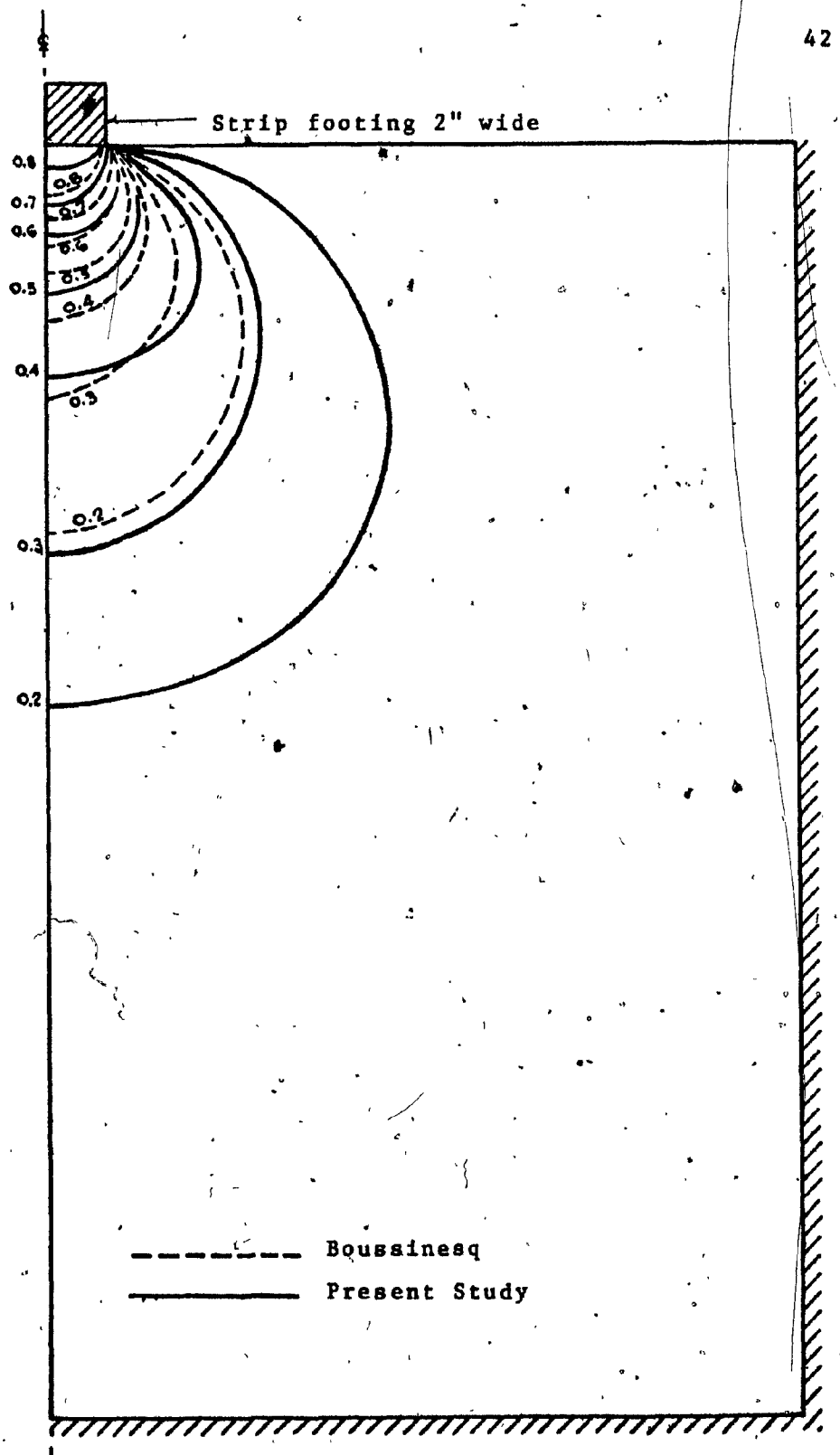

FIG. 15. STRESS DISTRIBUTION BENEATH THE FOOTING AT 20 PSI

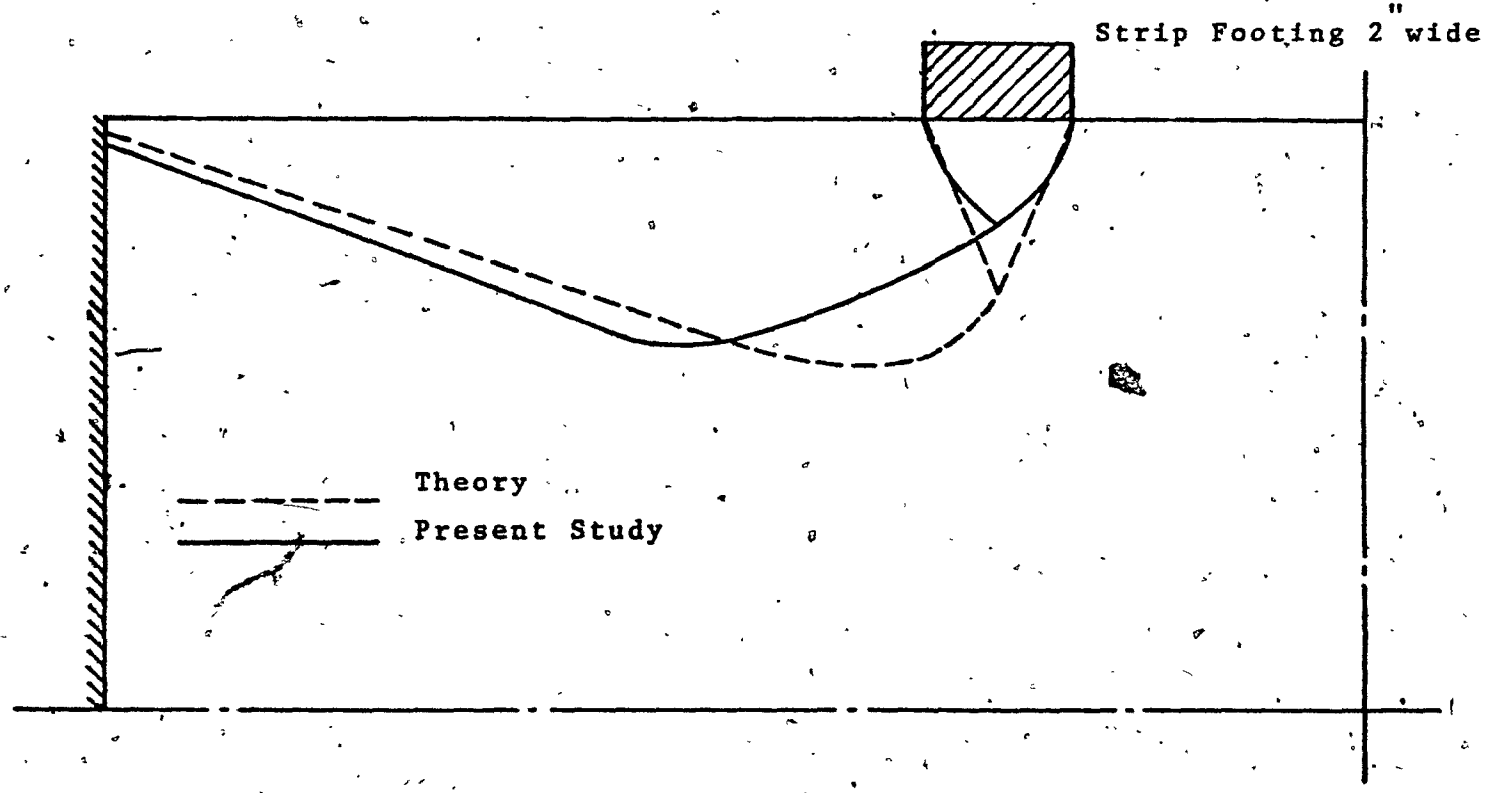

FIG. 16. PLANE OF FAILURE

Chapter 5

CONCLUSION

The results obtained by a finite element technique are compared with the existing theories and the experimental test results of Hanna. The value of the ultimate bearing capacity agreed with the test results when using plane strain values for the soil parameters. The disagreement in the settlement value is attributed to the difference between the strain controlled condition of the test and the stress controlled condition of the finite element. The stress bulbs beneath the footing disagreed with results obtained from Boussinesq theory at higher values than $\frac{1}{3} q_u$. A general shear failure mode was obtained as expected.

The use of triaxial test result in a plane strain problem will give a low value for the ultimate bearing capacity i.e. a higher factor of safety and a conservative design. When the value of ϕ_p is used instead of ϕ_t a 90% accuracy is obtained in the value of q_u.

The results obtained by finite element suggests that the method can be applied to more complicated problems in soil mechanics as the two layered soil problem.

REFERENCES

1- Bowles, J.E., (1977), "Foundation Analysis and Design". New York: Mc Graw-Hill Publishing Co.

2- Duncan, J.M., and Chang, C.Y. (1970), "Nonlinear Analysis of Stress and Strains in Soils", Journal of the Soil Mechanics and Foundations division, ASCE, Vol. 96 No. SM5, Sept., pp. 1629-1653.

3- Girijavallabhan, C.V., and Reese, L.C., (1968), "Finite Element Method for Problems in Soil Mechanics", Journal of the Soil Mechanics and Foundations Division, ASCE, Vol. 94, No. SM2, March, pp. 473-496.

4- Hanna, A.M., (1978), "Bearing Capacity of Footing Under Vertical and Inclined Loads on Layered Soils. Ph. D. Thesis, Nova Scotia Technical College, Halifax, N.S.

5- Kondner, R.L., (1963), "Hyperbolic Stress-Strain Response: Cohesive Soils", Journal of the Soil Mechanics and Foundations Division, ASCE, Vol. 89, No. SMI, pp. 115-143.

6- Kulhawy, F.H., and Duncan, J.M., (1972), "Stresses and Movements of Oroville Dan", Journal of the Soil Mechanics and Foundations Division, ASCE, Vol. 98, No. SM7 July, pp. 653-665.

7- Meyerhoff, G.G., and Hanna, A.M., (1978), "Ultimate Bearing Capacity of Foundations on Layered Soils Under Inclined Loads", Canadian Geotechnical Journal, Volume 15, No. 4, pp. 565-572.

8- Withiam, J.L., and Kulhawy, F.H., (1976), "Undrained Volume Changes in Compacted Cohesive Soil", Journal of the Soil Mechanics and Foundations Division, ASCE, Vol. 102, No. GT10, October, pp. 1029-1039.

9- Wu, T.H., (1976), "Soil Mechanics", Boston: Allyn and Bacon, Inc.

10- Zienkiewicz, O.C., (1976), "The Finite Element Method in Structural and Continuum Mechanics", New York: Mc Graw-Hill Publishing Co.

APPENDIX I

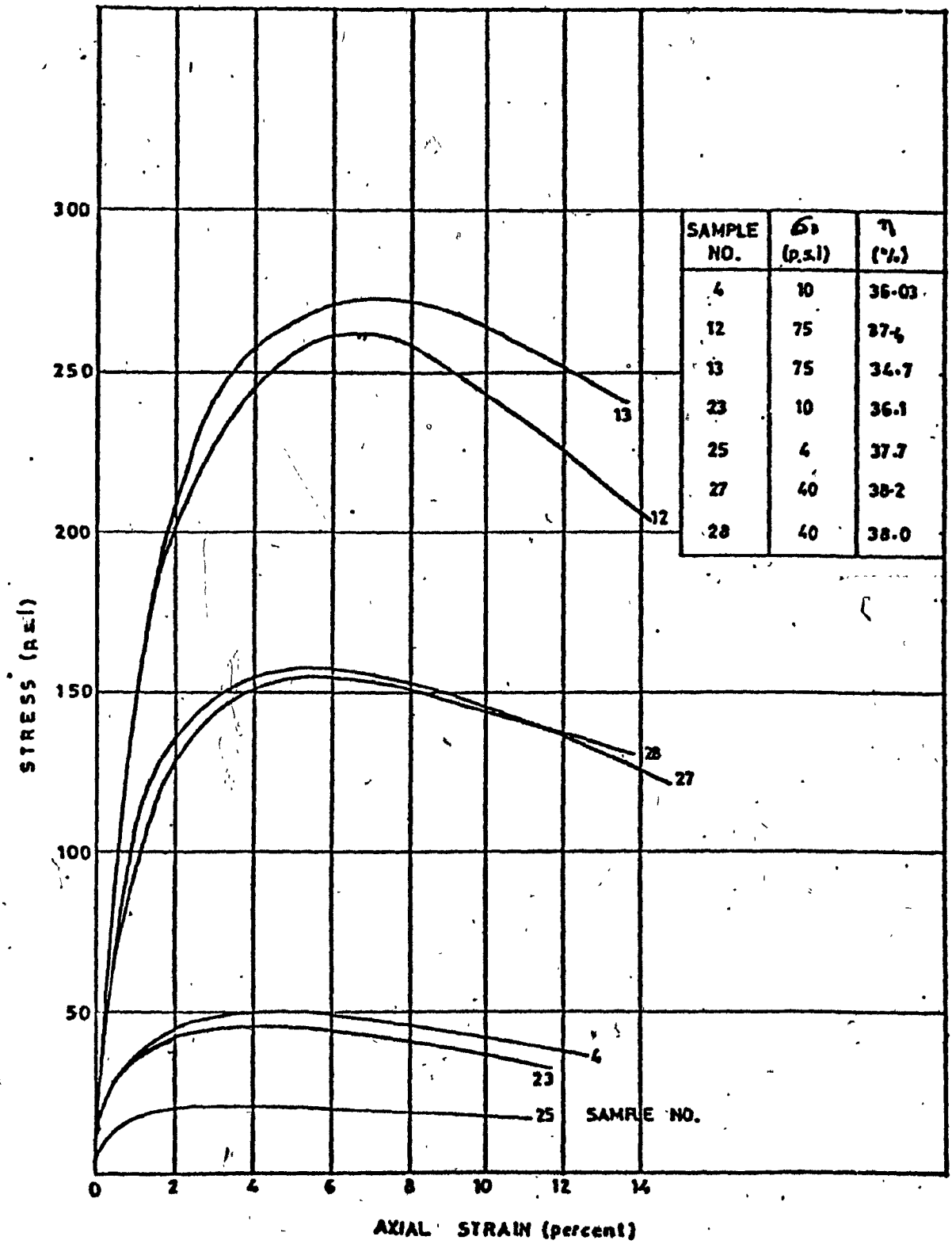

FIGURE I·2 EFFECT OF CELL PRESSURE ON STRESS STRAIN BEHAVIOUR OF DENSE SAND

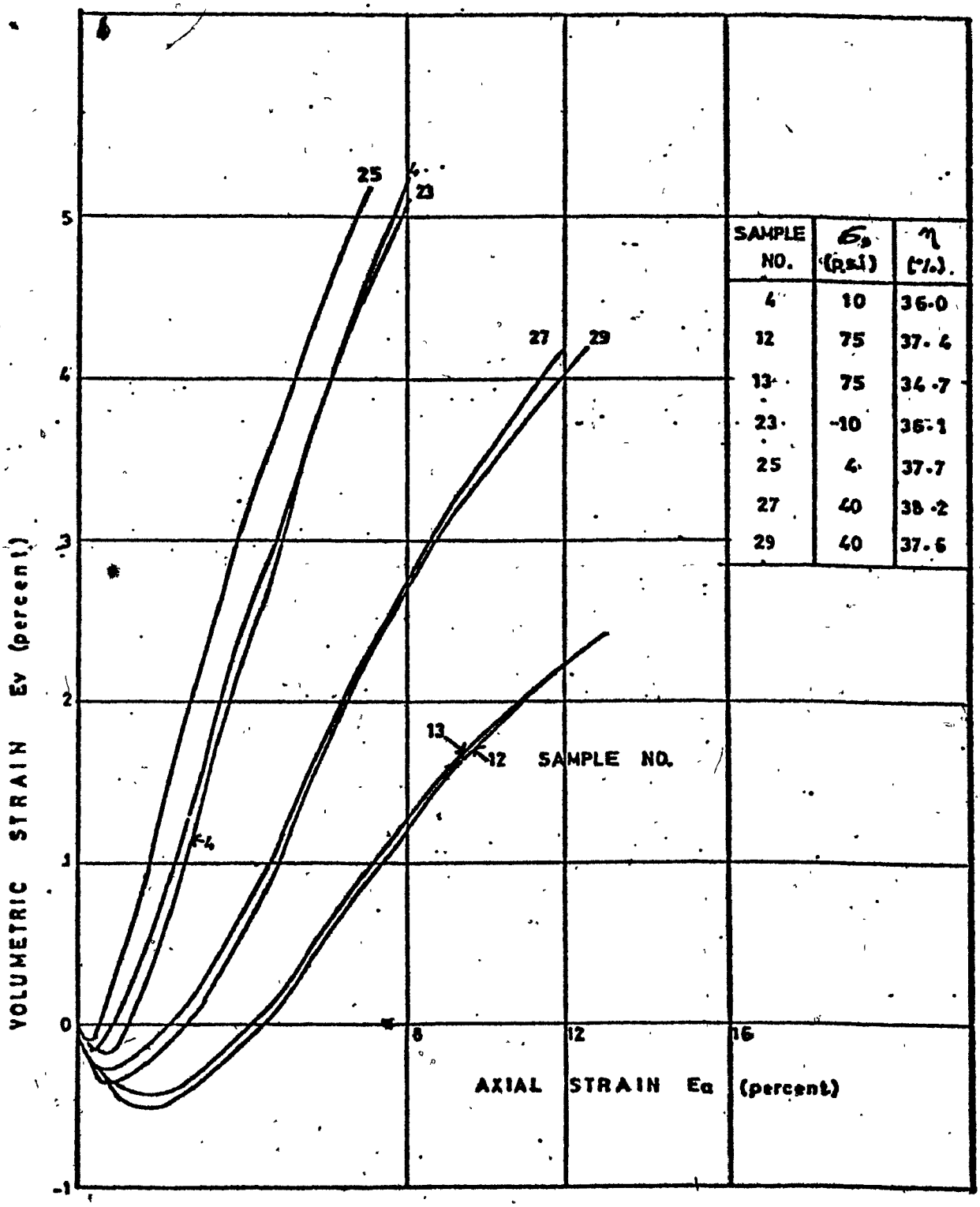

FIGURE I·3 EFFECT OF CELL PRESSURE ON VOLUMETRIC STRAIN OF DENSE SAND

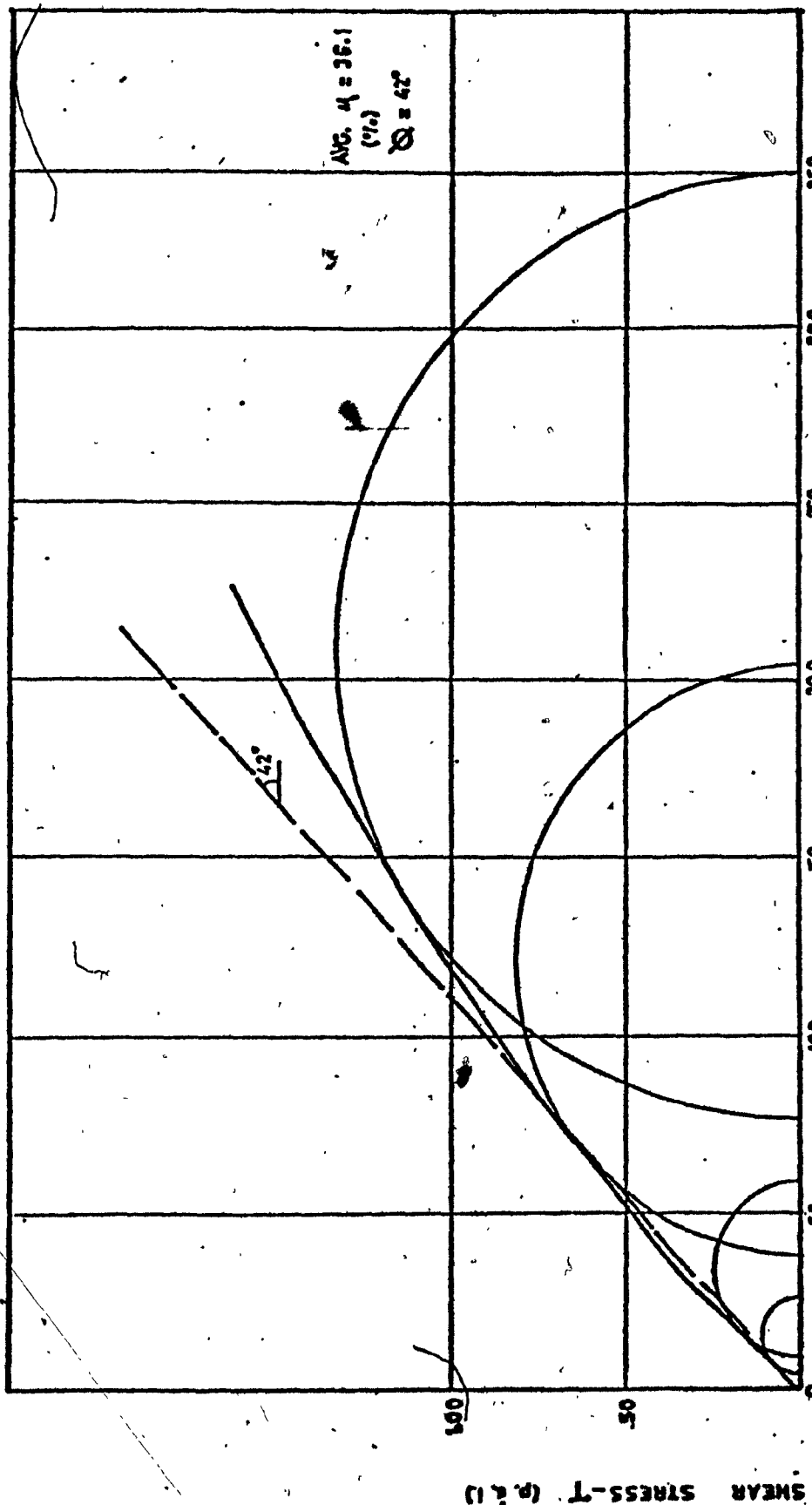

FIGURE 1.6 MOHR COULOMB ENVELOPE FOR DENSE SAND